Long-Range Order and Directional Defect Propagation in the Nonreciprocal *XY* Model with Vision Cone Interactions

Sarah A. M. Loos,[1,*] Sabine H. L. Klapp,[2] and Thomas Martynec[2]
[1]*DAMTP, Centre for Mathematical Sciences, University of Cambridge, Wilberforce Road, Cambridge CB3 0WA, United Kingdom*
[2]*Technische Universität Berlin, Straße des 17. Juni 135, 10623 Berlin, Germany*

(Received 23 June 2022; revised 1 December 2022; accepted 11 April 2023; published 9 May 2023)

We study a two-dimensional, nonreciprocal *XY* model, where each spin interacts only with its nearest neighbors in a certain angle around its current orientation, i.e., its "vision cone." Using energetic arguments and Monte Carlo simulations, we show that a true long-range ordered phase emerges. A necessary ingredient is a configuration-dependent bond dilution entailed by the vision cones. Strikingly, defects propagate in a directional manner, thereby breaking the parity and time-reversal symmetry of the spin dynamics. This is detectable by a nonzero entropy production rate.

DOI: 10.1103/PhysRevLett.130.198301

A growing number of papers demonstrate that nonreciprocal (NR) interactions which break the action-reaction principle are the origin of intriguing physical phenomena in nonequilibrium systems [1–9]. A prominent example is traveling-wave phases in binary fluids, which can be caused by NR coupling between the two fluid components [2,3]. These time-dependent phases break the $\mathcal{PT}$ symmetry of the system, and their emergence has been linked to the existence of underlying exceptional points [1]. In solids and soft crystals it was recently shown that NR interactions may introduce odd elasticity [4,5]. A common source of nonreciprocity in biological and artificial systems is perception within a finite *"vision cone,"* which naturally leads to interactions that are NR and orientation dependent. For example, which neighbors a pedestrian in a crowd [10], a car driver in a traffic jam [11], or a bird in a flock [12] reacts to may depend on its current orientation. The few studies on this subject in the area of motile active matter have shown that vision cone interactions can lead to the formation of new self-organized patterns and aggregates [13–16].

To gain deeper insights into the physical mechanisms induced by nonreciprocity, we study in this Letter how NR vision cone interactions affect the behavior of many-body systems on a lattice. Indeed, lattice models have proven invaluable to study fundamental questions of statistical physics, in particular concerning the emergence of phases and phase transitions, in addition to having numerous applications in physics, engineering, socioeconomics, and biology. Here, we implement vision cone interactions into the *XY* model with short-range coupling (Fig. 1), which allows us to study the interplay between a continuous rotational dynamics, alignment interactions, and vision cones. We uncover two intriguing phenomena. First, NR interactions can induce a true long-range ordered (LRO) phase. This is in sharp contrast to the standard short-ranged *XY* model, in which a LRO phase is forbidden by the Mermin-Wagner theorem. Remarkably, LRO even arises for vision cones that are almost 360°. Second, the vision cone interactions cause defects to propagate in a directional, parity-broken manner. This directional spin dynamics also breaks the time-reversal symmetry, which we measure by the entropy production rate (EPR). Indeed, we have recently shown that nonreciprocity generally causes EPR > 0 [6]. Here, we find that the EPR has a maximum close to the onset of the disordered (DO) phase. Using a NR version of the classical *XY* model enables us to rationalize these phenomena by adapting a language and toolbox well known from equilibrium statistical mechanics,

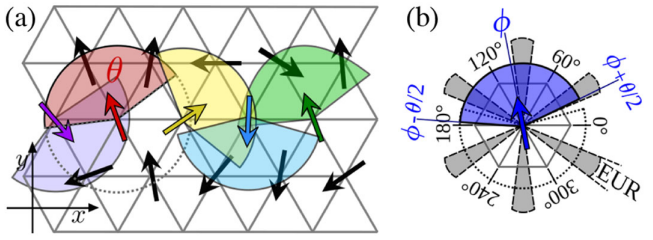

FIG. 1. (a) Illustration of the model on a hexagonal lattice. Each spin interacts only with those nearest neighbors lying in its vision cone of size θ. (b) If the spin orientation ϕ lies in the EUR (six gray shaded regions), the total number of coupled neighbors is reduced by one.

including spin wave excitation, energy minimization, and bond percolation.

Model.—We consider a two-dimensional lattice of spins $S_i \in \mathbb{R}^2$, $i \in \{1, 2, \ldots, L^2\}$, whose orientations $\phi_i \in [0, 360°)$ can continuously rotate in the lattice plane. All spins are connected to a heat bath at temperature T. The total energy of the system is $E_{\mathrm{tot}} = \sum_i E_i$, with

$$E_i = -\sum_{\langle j \rangle} J_{ij}(\phi_i) \cos(\phi_i - \phi_j), \tag{1}$$

where the sum runs over all nearest-neighboring lattice sites of i. Different from the standard XY model, the coupling constant J_{ij} explicitly depends on the orientation of S_i and the lattice position of S_j, since only neighbors within the vision cone of size $\theta \in (0, 360°]$ are coupled; namely,

$$J_{ij}(\phi_i) = \begin{cases} J & \min\{360° - |\phi_i - \vartheta_{ij}|, |\phi_i - \vartheta_{ij}|\} \leq \frac{\theta}{2} \\ 0 & \text{else,} \end{cases} \tag{2}$$

where $\vartheta_{ij} \in \{k360°/n\}$, $k \in \{1, \ldots, n\}$ denotes the angle of the connecting line between S_i and S_j, with n being the number of nearest neighbors per spin. As typical representatives for two-dimensional lattice geometries, we consider the hexagonal lattice (where $n = 6$) and the square lattice ($n = 4$). In the theoretical considerations, we however do not specify the lattice geometry, so that our results are more general.

We investigate the spin-flip dynamics by Monte Carlo simulations with Glauber transition rates [17] $w(\phi_i \to \phi_i') = (1 - \tanh\{[E_i(\phi_i) - E_i(\phi_i')]/2T\})/2$, with the Boltzmann constant set to unity, and apply periodic boundary conditions. We set J to 1 (ferromagnetic coupling). For $\theta = 360°$, the model reduces to the standard XY model. For $\theta < 360°$, the coupling matrix $\mathbf{J}$ with elements J_{ij} [Eq. (2)] is generally asymmetric, meaning that the coupling between two spins may be NR, $J_{ij} \neq J_{ji}$. In particular, some bonds are unidirectional ($J_{ij} \neq 0$, but $J_{ji} = 0$), and some bonds are missing ($J_{ij} = J_{ji} = 0$). Furthermore, $\mathbf{J}$ is configuration dependent. From the viewpoint of network science, this is a dynamic or temporal network and, due to the presence of NR links, a *directed* graph. However, the fact that $\mathbf{J}$ is a function of the orientations $\{\phi_i(t)\}$ crucially differentiates our model from other spin models on directed graphs [18–20]. Here, the spin dynamics and network structure are mutually interrelated.

Phase behavior.—The standard XY model ($\theta = 360°$) displays a low-temperature quasi-long-range ordered (QLRO) phase that crosses at high temperatures by an infinite-order Berezinskii-Kosterlitz-Thouless (BKT) transition to a disordered phase. Our most striking finding is that for vision cone sizes $\theta < 360°$, a LRO ferromagnetic phase at finite T emerges, for both lattice geometries. The LRO phase is marked by an average magnetization $\langle m \rangle \to 1$ and a large spin-spin correlation $\langle S_i S_{i+d} \rangle$ that spans the entire system (Fig. 2). Averages $\langle \cdot \rangle$ are taken over all spins and multiple realizations. For both lattices, the LRO is absent, if θ is a multiple of $(360°/n)$ (i.e., a multiple of 60° for the hexagonal, or of 90° for the square lattice). Besides this, the phase behavior and related transitions differ between both lattices. On the hexagonal lattice, the system displays a QLRO phase in between the LRO and DO phase, marked by algebraically decaying $\langle S_i S_{i+d} \rangle$. (In the Supplemental Material, we also consider a second measure to distinguish the phases [21].) We detect traces of two corresponding transitions in the form of two peaks in the specific heat, $C_v = L^2(\langle E_{\mathrm{tot}}^2 \rangle - \langle E_{\mathrm{tot}} \rangle^2)/T^2$ [Figs. 2(d) and 2(f)]. The peak heights and positions do not scale with the system size, suggesting that both transitions are of infinite order. On the square lattice, we do not detect a QLRO phase (unless $\theta/90° \in \mathbb{N}$; see below). The order-disorder transition on the square lattice is marked by peaks in C_v that increase with L, indicating critical behavior [Fig. 2(k)]. (The higher moments of m, concretely the Binder cumulants and susceptibility, also express behavior typical of second-order phase transitions; see Ref. [21].) For the special cases $\theta/(360°/n) \in \mathbb{N}$, we detect on both lattices a QLRO and a DO phase, reminiscent of the standard XY model.

To understand this nonequilibrium phase behavior, one feature of the vision cone interactions turns out to be especially important. Namely, the *total number* of neighbors S_j of a spin S_i for which $J_{ij} \neq 0$ is generally configuration dependent. In particular, the number is reduced by one, if ϕ_i lies in what we call the "energetically unfavorable range" (EUR). The EUR nullifies for $\theta/(360°/n) \in \mathbb{N}$ and otherwise consists of n angular regions [gray areas in Fig. 1(b)] which in total amount to an angle of $n\{(360°/n) - [\theta \bmod (360°/n)]\}$. In a LRO configuration, E_{tot} is invariant under global rotation of all spins, but only as long as the rotation does not bring $\langle \phi_i \rangle$ in the EUR. Thus, the rotational U(1) symmetry of the system is in general broken. Still, the ground state is generally infinitely degenerate. If the EUR nullifies, the U(1) symmetry is restored.

Based on energetic considerations, we can now explain the emergence or absence of LRO for different θ. Consider a fully ordered system. In the standard XY model, the energy required to rotate a spin S_i by a small angle ψ_i is $\mathcal{E}_i \sim \psi_i^2$, which follows from Eq. (1). In contrast, if $\theta < 360°$, the number of bonds can change, yielding $\mathcal{E}_i \sim \psi_i^2 + J$ if the spin enters the EUR due to the rotation, and $\mathcal{E}_i \sim \psi_i^2$ else. Rotating all spins by an angle $\psi = 2\pi/L$ with respect to their neighbor in one given spatial direction forms the spin wave of longest wavelength that fully destroys the orientational order (Fig. 3). In cases where the EUR nullifies, the excitation of such a spin wave takes an energy increase of $\mathcal{E}_{\mathrm{tot}} = \sum_i \mathcal{E}_i = L^2 4\pi^2/L^2 = 4\pi^2$, which is finite even in the thermodynamic limit $L \to \infty$.

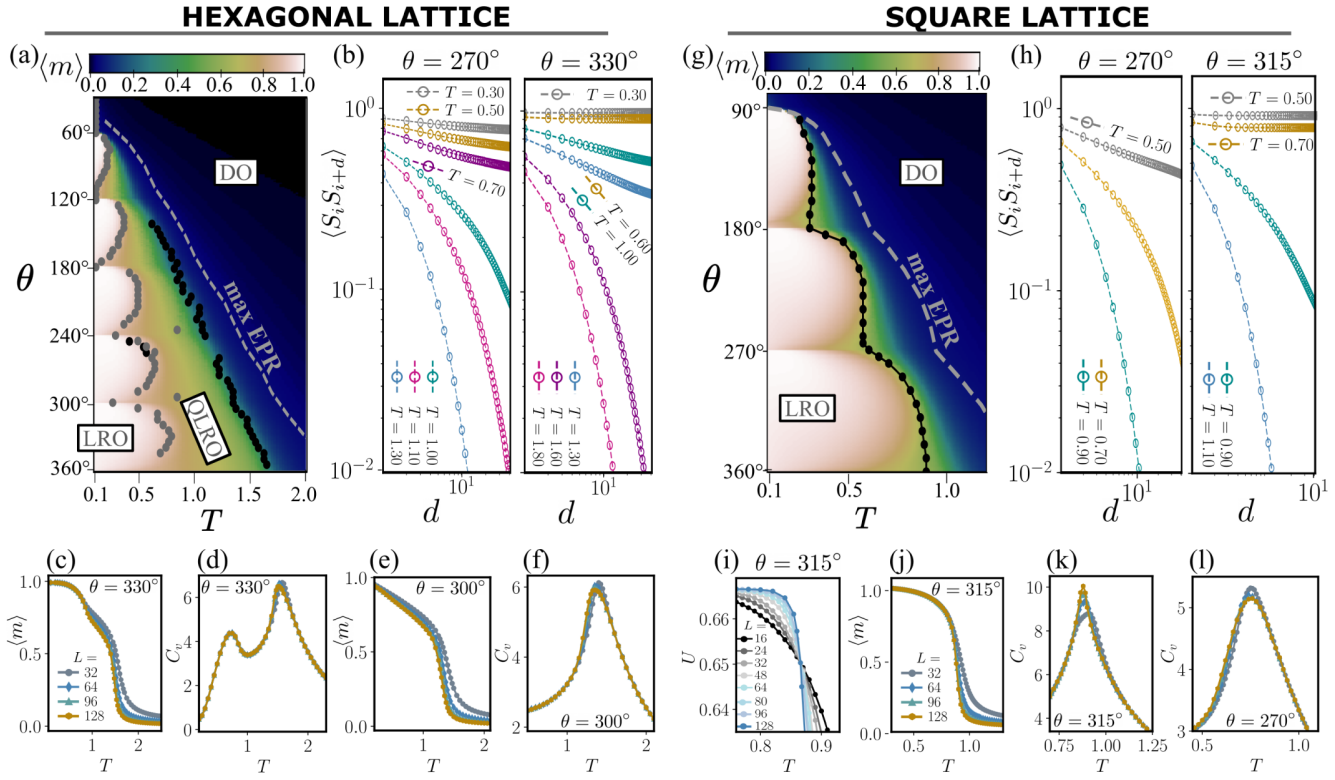

FIG. 2. (a)–(f) Hexagonal lattice. (a) Average of magnetization $m = \sqrt{(\sum \cos\phi_i)^2 + (\sum \sin\phi_i)^2}/L^2$ as function of T and θ. (b) Decay of spin-spin correlations $\langle S_i S_{i+d}\rangle$ with distance d for $\theta = 270°$ and $\theta = 330°$ ($L = 192$). (c),(d) $\langle m\rangle(T)$ and $C_v(T)$ for $\theta = 330°$ and various system sizes L. (e),(f) $\langle m\rangle$ and C_v for $\theta = 300°$. The black and gray symbols in (a) depict the positions of the peaks in C_v and are rough estimators for the positions of the phase boundaries. (g)–(l) Square lattice. (g) Magnetization map and (h) spin-spin correlations. The black symbols in (g) show the LRO-DO transition temperatures estimated from the crossing of the Binder cumulants $U = 1 - (\langle m^4\rangle/3\langle m^2\rangle^2)$. (i)–(k) U, $\langle m\rangle$, and C_v for $\theta = 315°$. (l) C_v for $\theta = 270°$.

Thus, thermal noise at any nonzero T can excite this mode and LRO is found only at $T \to 0$. In contrast, if $\theta/(360°/n) \notin \mathbb{N}$,

$$\mathcal{E}_{\text{tot}} = L^2(4\pi^2/L^2 + \eta J) = 4\pi^2 + L^2\eta J, \tag{3}$$

with $\eta \in [0, 1)$ denoting the fraction of spins that enter the EUR by the rotation. For large L, η approaches

$$\eta \to 1 - [\theta \bmod (360°/n)]/(360°/n), \tag{4}$$

which is independent of L. The energetic cost of forming a spin wave [Eq. (3)] thus *diverges* for $L \to \infty$. For large enough systems, this mode cannot be excited by noise and therefore does not destabilize the ground state.

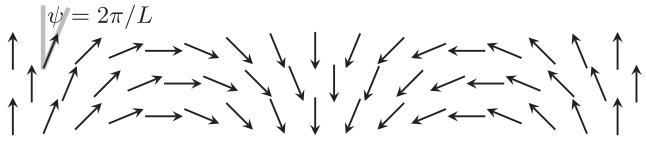

FIG. 3. Spin wave of longest wavelength and lowest energy that fully destroys the order in x direction. Here, $L = 17$.

This rationalizes the emergence of a LRO phase for $\theta/(360°/n) \notin \mathbb{N}$. This argument also explains why the nonreciprocity alone does not suffice for LRO.

Also the emergence and absence of the QLRO on the hexagonal versus square lattice [for $\theta/(360°/n) \notin \mathbb{N}$], respectively, can be rationalized from the EUR. Specifically, for low temperatures, the EUR effectively restricts the accessible spin orientations to n angular regions. A quasidiscretized spin dynamics with 4 effective states does not provide sufficient rotational freedom to form a QLRO with its typical topological defects, while 6 states suffices. See Ref. [21] for more details.

Another observation is the general absence of (Q)LRO phases for narrow cones, $\theta < (360°/n)$. This can be explained by a bond percolation argument. The main point is that, as it is well known from bond-diluted, standard XY models, the bond concentration p must be above the bond percolation threshold p_c to form (Q)LRO for finite T [31–36]. Otherwise, the ground state may comprise disjoint, noninteracting clusters, whose orientations are independent from each other, preventing global ordering. Here, for vision cones $\theta < (360°/n)$, the total fraction of bonds p does not exceed the respective bond peculation

threshold, which is $p_c = 2\sin(\pi/18) \approx 0.347$ for the hexagonal and $p_c = 1/2$ for the square lattice [37]. (Specifically, $p \in [0, 1/3]$ for the hexagonal, and $p \in [0, 1/2]$ for the square lattice [21].) Remarkably, it is not the concentration of bidirectional bonds $p_{\rm bi}$ (where $J_{ij} \neq 0$ *and* $J_{ji} \neq 0$) that matters. (Indeed, $p_{\rm bi} > p_c$ only holds for $\theta \geq 240°$ on the hexagonal and $\theta \geq 270°$ on the square lattice [21].) Rather, a total bond concentration p of bidirectional plus unidirectional bonds above p_c suffices. This is in sharp contrast to bond-diluted spin models on random, directed graphs [20]. This is because, in our model, the existence or absence of each bond is not random, but determined by the spin orientations. In the LRO phase, the system self-organizes such that exactly those bonds are present that are needed for percolation.

Next, we consider the θ dependence of the transition temperatures. First, as θ decreases, the transition to DO is overall shifted toward lower T (Fig. 2). This suits to the fact that p decreases with θ. Indeed, for the reciprocal bond-diluted XY model, the BKT transition is known to decrease with p [36]. Next, the low-temperature transition from LRO to QLRO or DO depends nonmonotonically on θ. Although this is a nonequilibrium system, the trend can be rationalized by considering the balance of energy and configuration entropy. First, the ground state energy decreases with decreasing θ, and the transition temperature is thus reduced. Second, for θ values between two multiples of $(360°/n)$, p and thus the energy of the fully ordered ground state are independent of θ. However, here the EUR increases linearly with decreasing θ. Assuming that the entropy is a logarithmic function of the number of accessible microstates (i.e., spin orientations) in the ground state, this implies that the entropic freedom due to spin rotation is decreasing logarithmically. Correspondingly, the transition temperature is lowest close to the θ values, where the EUR is largest (see Ref. [21] for illustrations).

Time-reversal symmetry breaking.—It was recently established that NR interactions can induce stable time-dependent phases, such as traveling waves [1–3]. These phases emerge in systems that comprise two distinct species with a "run-and-catch" or "prey-predator" relation, i.e., one species is attracted or aligning to the other, while the reverse interaction is repulsive or antialigning. In contrast, our model comprises only a *single* species of constituents who all interact with each other in an identical manner. We do not observe time-dependent phases, and all emergent phases have an equilibrium counterpart. However, we find that the spin dynamics clearly reveals the far-from-equilibrium character of the system. In particular, we observe long-lived (yet transient) directional propagation of local heterogeneous spin structures, e.g., defects. To visualize the directional propagation, we start from a fully ordered configuration in the LRO phase and introduce two defect lines; see Fig. 4. In marked contrast to an equilibrium system, where the defects would diffuse in all spatial directions, the defect lines propagate in a preferred spatial direction, which is dictated by the spin orientations. The underlying reason is that the defect is "visible" only to the spins facing it, meaning that the information travels only in certain spatial directions. Despite the spatial symmetry of the initial bands (here, the parity symmetry $y \to -y$), the response of the system is strongly asymmetric, and breaks the parity. Because of the predetermined propagation, the initiated spin dynamics moreover clearly breaks the *time-reversal symmetry*. If the video was played backward, the defect lines would move in the "wrong" direction. The initiated "traveling wave" survives a considerable period of time (for Fig. 4, the defects travel ∼10 times over L before dissolving). Eventually, the system collectively reorganizes into a LRO state which lacks global currents.

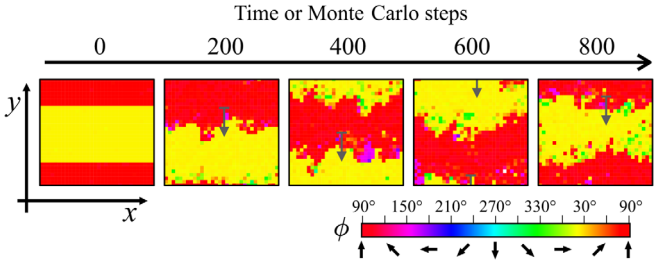

FIG. 4. Illustration of defect propagation. Leftmost panel: initial configuration with spin orientations $\phi = 30°$ in the yellow middle band, and $\phi = 90°$ else. The two interfaces (defect lines) propagate downward as shown in the consecutive panels. Here, $L = 32$, $T = 0.1$, $\theta = 65°$, hexagonal lattice.

This mechanism leads to directional spin fluctuations in all three phases. The resulting time-reversal symmetry breaking can be quantified by the mean entropy production rate per spin, which we numerically evaluate using a formula from stochastic thermodynamics [38–41]:

$$\mathrm{EPR} = \left\langle \ln \frac{w[\phi_i(t) \to \phi_i(t+dt)]}{w[\phi_i(t+dt) \to \phi_i(t)]} \right\rangle / dt. \tag{5}$$

We find a strictly positive EPR in all phases (Fig. 5). This is true for all $\theta < 360°$, even when the EUR vanishes and the number of bonds is constant [Fig. 5(b)]. Interestingly,

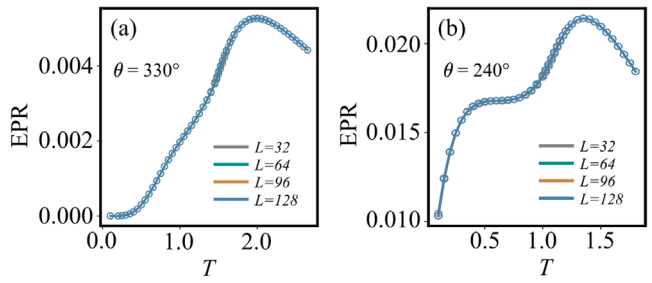

FIG. 5. Entropy production rate [Eq. (5)] versus T on the hexagonal lattice with (a) $\theta = 330°$ and (b) $\theta = 240°$. $L = 192$.

the EPR has a pronounced maximum, which always lies within and close to the onset of the DO phase. The location of this maximum for all θ is shown in Figs. 2(a) and 2(g) by gray dashed lines. The maximum can be explained by the competition of two effects. In view of the directional propagation of defects, which we identified as a source of time-reversal symmetry breaking, it makes sense that the EPR generally increases with T, simply because the defect density increases. This also explains why the increase of EPR is particularly steep around the transitions. On the other hand, the defect density eventually saturates in the DO phase, and the orientation of each spin decorrelates with its local environment. Upon a further raise of T, the noise then only dominates more over the increasingly irrelevant alignment interactions and thus overshadows the propagation mechanism. The result is an ultimately purely random motion—which is time symmetric. Lastly, we note that the slope of EPR has a similar behavior as C_v [21], which was also observed in Refs. [38,40,41].

Discussion.—We provide numerical evidence and analytical reasoning demonstrating that NR vision cone interactions can lead to the emergence of a LRO phase in a two-dimensional model of continuous spins with short-range coupling. The nonreciprocity alone is not sufficient, but the orientation-dependent bond dilution is crucial. Furthermore, the nature of the phase transitions is different on the square and hexagonal lattice. Interestingly, in a coarse-grained model with NR coupling and spin inertia, the theoretical existence of LRO was recently shown on a hydrodynamic level [42], suggesting an alternative mechanism to introduce LRO in NR systems. We further found that local heterogeneous spin structures travel with a preferred direction. Somewhat analogously, NR interactions in (soft) crystals can turn topological defects in the crystalline structure into motile objects [4,5]. Since the here described mechanism is specific to the vision cone interactions, a further investigation of the relation between both phenomena could yield valuable insights. We have also studied the time-reversal symmetry breaking of the spin dynamics by the EPR, and found a maximum close to the transition to DO. To obtain a more profound understanding it could be worthwhile to investigate the formation, annihilation, and motion of vortex-antivortex pairs. Another interesting research perspective concerns the relation to motile active matter. The directional propagation of defects and information described here could have a drastic impact on flock cohesion and collective turns [8,43].

This work was funded by the Deutsche Forschungs gemeinschaft (DFG, German Research Foundation) through Projects No. 498288081 and No. 163436311-SFB 910. We thank Benjamin Walter, Asja Jelić, Gianmaria Falasco, Jaron Kent-Dobias, Cesare Nardini, Tal Agranov, and Michel Fruchart for valuable comments.

*sl2127@cam.ac.uk

[1] M. Fruchart, R. Hanai, P. B. Littlewood, and V. Vitelli, Nonreciprocal phase transitions, Nature (London) **592**, 363 (2021).
[2] Z. You, A. Baskaran, and M. C. Marchetti, Nonreciprocity as a generic route to traveling states, Proc. Natl. Acad. Sci. U.S.A. **117**, 19767 (2020).
[3] S. Saha, J. Agudo-Canalejo, and R. Golestanian, Scalar Active Mixtures: The Nonreciprocal Cahn-Hilliard Model, Phys. Rev. X **10**, 041009 (2020).
[4] L. Braverman, C. Scheibner, B. VanSaders, and V. Vitelli, Topological Defects in Solids with Odd Elasticity, Phys. Rev. Lett. **127**, 268001 (2021).
[5] A. Poncet and D. Bartolo, When Soft Crystals Defy Newton's Third Law: Nonreciprocal Mechanics and Dislocation Motility, Phys. Rev. Lett. **128**, 048002 (2022).
[6] S. A. M. Loos and S. H. L. Klapp, Irreversibility, heat and information flows induced by non-reciprocal interactions, New J. Phys. **22**, 123051 (2020).
[7] M. Brandenbourger, X. Locsin, E. Lerner, and C. Coulais, Non-reciprocal robotic metamaterials, Nat. Commun. **10**, 4608 (2019).
[8] A. Cavagna, I. Giardina, A. Jelic, S. Melillo, L. Parisi, E. Silvestri, and M. Viale, Nonsymmetric Interactions Trigger Collective Swings in Globally Ordered Systems, Phys. Rev. Lett. **118**, 138003 (2017).
[9] A. V. Ivlev, J. Bartnick, M. Heinen, C.-R. Du, V. Nosenko, and H. Löwen, Statistical Mechanics where Newton's Third Law Is Broken, Phys. Rev. X **5**, 011035 (2015).
[10] A. Nicolas and F. H. Hassan, Social groups in pedestrian crowds: Review of their influence on the dynamics and their modelling, Transportmetrica A **19**, 1 (2021).
[11] W. Knospe, L. Santen, A. Schadschneider, and M. Schreckenberg, Towards a realistic microscopic description of highway traffic, J. Phys. A **33**, L477 (2000).
[12] A. Nathan and V. C. Barbosa, V-like formations in flocks of artificial birds, Artif. Life **14**, 179 (2008).
[13] L. Barberis and F. Peruani, Large-Scale Patterns in a Minimal Cognitive Flocking Model: Incidental Leaders, Nematic Patterns, and Aggregates, Phys. Rev. Lett. **117**, 248001 (2016).
[14] M. Durve, A. Saha, and A. Sayeed, Active particle condensation by non-reciprocal and time-delayed interactions, Eur. Phys. J. E **41**, 49 (2018).
[15] A. Costanzo, Milling-induction and milling-destruction in a Vicsek-like binary-mixture model, Europhys. Lett. **125**, 20008 (2019).
[16] F. A. Lavergne, H. Wendehenne, T. Bäuerle, and C. Bechinger, Group formation and cohesion of active particles with visual perception-dependent motility, Science **364**, 70 (2019).
[17] J. Marro and R. Dickman, *Nonequilibrium Phase Transitions in Lattice Models* (Cambridge University Press, Cambridge, England, 1999).
[18] F. Lima and D. Stauffer, Ising model simulation in directed lattices and networks, Physica (Amsterdam) **359A**, 423 (2006).
[19] A. D. Sánchez, J. M. López, and M. A. Rodriguez, Nonequilibrium Phase Transitions in Directed Small-World Networks, Phys. Rev. Lett. **88**, 048701 (2002).

[20] A. Lipowski, A. L. Ferreira, D. Lipowska, and K. Gontarek, Phase transitions in Ising models on directed networks, Phys. Rev. E **92**, 052811 (2015).
[21] See Supplemental Material at http://link.aps.org/supplemental/10.1103/PhysRevLett.130.198301, which includes Refs. [22–30], for additional numerical results and a detailed description of the ground states and bond dilution. It also sketches a possible free-energy argument for the stability of the LRO.
[22] S. K. Baek, P. Minnhagen, and B. J. Kim, True and quasi-long-range order in the generalized q-state clock model, Phys. Rev. E **80**, 060101(R) (2009).
[23] K. Binder, Finite size scaling analysis of Ising model block distribution functions, Z. Phys. B **43**, 119 (1981).
[24] J. M. Kosterlitz and D. J. Thouless, Ordering, metastability and phase transitions in two-dimensional systems, J. Phys. C **6**, 1181 (1973).
[25] J. M. Kosterlitz, The critical properties of the two-dimensional XY model, J. Phys. C **7**, 1046 (1974).
[26] F.-Y. Wu, The Potts model, Rev. Mod. Phys. **54**, 235 (1982).
[27] M. Nauenberg and D. Scalapino, Singularities and Scaling Functions at the Potts-Model Multicritical Point, Phys. Rev. Lett. **44**, 837 (1980).
[28] H. Duminil-Copin, V. Sidoravicius, and V. Tassion, Continuity of the phase transition for planar random-cluster and Potts models with $1 \leq q \leq 4$, Commun. Math. Phys. **349**, 47 (2017).
[29] N. P. Kryuchkov, E. V. Yakovlev, E. A. Gorbunov, L. Couëdel, A. M. Lipaev, and S. O. Yurchenko, Thermoacoustic Instability in Two-Dimensional Fluid Complex Plasmas, Phys. Rev. Lett. **121**, 075003 (2018).
[30] T. Surungan, S. Masuda, Y. Komura, and Y. Okabe, Berezinskii-Kosterlitz-Thouless transition on regular and Villain types of q-state clock models, J. Phys. A **52**, 275002 (2019).
[31] B. Berche, A. Farinas-Sanchez, Y. Holovatch, and R. Paredes, Influence of quenched dilution on the quasi-long-range ordered phase of the 2d XY model, Eur. Phys. J. B **36**, 91 (2003).
[32] Y. Okabe and T. Surungan, Phase transition of two-dimensional diluted XY and clock models, Prog. Theor. Phys. Suppl. **157**, 132 (2005).
[33] B. Costa, L. Lima, P. Z. Coura, S. Leonel, and A. Lima, Kosterlitz-Thouless transition: The diluted XY model, in *Journal of Physics: Conference Series* (IOP Publishing, João Pessoa, Brazil, 2014), Vol. 487, p. 012008.
[34] M. Kumar, S. Chatterjee, R. Paul, and S. Puri, Ordering kinetics in the random-bond XY model, Phys. Rev. E **96**, 042127 (2017).
[35] O. Kapikranian, Spin-spin correlation function of the two-dimensional XY model with weak site or bond dilution, Phys. Rev. B **85**, 094405 (2012).
[36] T. Surungan and Y. Okabe, Kosterlitz-Thouless transition in planar spin models with bond dilution, Phys. Rev. B **71**, 184438 (2005).
[37] M. F. Sykes and J. W. Essam, Exact critical percolation probabilities for site and bond problems in two dimensions, J. Math. Phys. (N.Y.) **5**, 1117 (1964).
[38] T. Tomé and M. J. de Oliveira, Entropy Production in Nonequilibrium Systems at Stationary States, Phys. Rev. Lett. **108**, 020601 (2012).
[39] J. Schnakenberg, Network theory of microscopic and macroscopic behavior of master equation systems, Rev. Mod. Phys. **48**, 571 (1976).
[40] C. E. Fernández Noa, P. E. Harunari, M. J. de Oliveira, and C. E. Fiore, Entropy production as a tool for characterizing nonequilibrium phase transitions, Phys. Rev. E **100**, 012104 (2019).
[41] T. Martynec, S. H. L. Klapp, and S. A. M. Loos, Entropy production at criticality in a nonequilibrium Potts model, New J. Phys. **22**, 093069 (2020).
[42] L. P. Dadhichi, J. Kethapelli, R. Chajwa, S. Ramaswamy, and A. Maitra, Nonmutual torques and the unimportance of motility for long-range order in two-dimensional flocks, Phys. Rev. E **101**, 052601 (2020).
[43] A. Attanasi, A. Cavagna, L. Del Castello, I. Giardina, T. S. Grigera, A. Jelić, S. Melillo, L. Parisi, O. Pohl, E. Shen *et al.*, Information transfer and behavioural inertia in starling flocks, Nat. Phys. **10**, 691 (2014).